DNA–Protein Interactions

International Edition: DOI: 10.1002/anie.201810373
German Edition: DOI: 10.1002/ange.201810373

Mechanism of DNA-Induced Phase Separation for Transcriptional Repressor VRN1

Huabin Zhou, Zihan Song, Sheng Zhong, Linyu Zuo, Zhi Qi, Li-Jia Qu,* and Luhua Lai**

Abstract: *Phase separation of proteins/nucleic acids to form non-membrane organelles is crucial in cellular gene-expression regulation. However, little is known about transcriptional regulator phase separation and the underlying molecular mechanism. Vernalization 1 (VRN1) encodes a crucial transcriptional repressor involved in plant vernalization that contains two B3 DNA-binding domains connected by an intrinsic disorder region (IDR) and nonspecifically binds DNA. We found that the Arabidopsis VRN1 protein undergoes liquid–liquid phase separation (LLPS) with DNA that is driven by multivalent protein–DNA interactions (LLPS), and that both B3 domains are required. The distribution of charged residues in the VRN1 IDR modulates the interaction strength between VRN1 and DNA, and changes in the charge pattern lead to interconversion between different states (precipitates, liquid droplets, and no phase separation). We further showed that VRN1 forms puncta in plant cell nuclei, suggesting that it may stabilize the vernalized state by repressing gene expression through LLPS.*

Genetic information encoded in DNA is tightly regulated through high-dimensional chromatin organization in the nucleus. Chromatin remodeling is a fundamental determinant of cell fate and cell identity.[1,2] It has been shown that transcriptional enhancers can mediate DNA phase separation that leads to super activation of gene expression.[3,4] Phase separation mediated by HP1α was associated with heterochromatin establishment and gene repression.[5,6] Condensation of the C-terminal tail of histone H1 has been shown to alter the assembly of DNA, which may be important for chromatin assembly and transcription regulation.[7] Spatiotemporal regulation of gene expression is essential for the determination of cell fate and identity, and thus for normal plant or animal development. However, it was unknown whether transcriptional regulators repress gene expression through phase-separation-mediated chromatin compaction and the underlying molecular mechanism.

The sequestration of molecules in a condensed phase efficiently alters their activity and stability, thereby facilitating signal transduction and stress response.[8,9] Multivalent interactions and intrinsic disorder regions (IDRs) are considered essential for phase separation.[10–12] Increases in binding valency and interaction strength facilitate phase separation and affect complex relaxation.[13–15] The interconversion between liquid and precipitate states is important in gene regulation, and is associated with various neurodegenerative diseases.[9,16,17]

Many flowering plants undergo vernalization after long-term exposure to cold during the winter, which causes changes in the chromatin structure of the flowering repressor gene *Flowering Locus C* (*FLC*). These cold-induced structural changes lead to *FLC* repression. Vernalization 1 (VRN1) is a key protein required for stable silencing of *FLC*.[18–20] Altered expression of VRN1 was associated with several plant morphological defects, thus suggesting that VRN1 is involved in plant development,[20,21] possibly by regulating the expression of other genes in addition to *FLC*. VRN1 contains two B3 DNA-binding domains flanked by an IDR that contains 115 residues (Figure 1a). Unlike other B3 family proteins, VRN1 displays nonspecific DNA binding in vitro.[18] The underlying molecular mechanism of VRN1-mediated *FLC* repression was still unknown.

We expressed the full-length *Arabidopsis* VRN1 in *Escherichia coli*, purified the VRN1 protein, and suspended it in HEPES buffer (see Figure S1 in the Supporting Information). Titration of the purified VRN1 with dsDNA FLC55 (55 base pairs (bp) upstream of the *FLC* promoter) led to the formation of spherical liquidlike droplets, which underwent fusion in a few seconds (Figure 1b). At a given protein concentration, the number and size of these droplets depended on the DNA concentration (see Figure S2).

To confirm that the observed droplets were liquidlike, we labeled VRN1 and the FLC55 DNA with engineered monomeric enhanced green fluorescent protein (EGFP) and Cyanine 5 (Cy5), respectively. The labeled VRN1 and FLC55 DNA formed droplets in a similar way to the unlabeled sample (see Figure S3). VRN1 and FLC55 colo-

[*] H. Zhou, Prof. L. Lai
BNLMS, State Key Laboratory for Structural Chemistry of Unstable and Stable Species, Peking-Tsinghua Center for Life Sciences
College of Chemistry and Molecular Engineering, Peking University
Beijing 100871 (P. R. China)
E-mail: lhlai@pku.edu.cn

H. Zhou, L. Zuo, Prof. Z. Qi, Prof. L. Lai
Center for Quantitative Biology
Peking-Tsinghua Center for Life Sciences
Academy for Advanced Interdisciplinary Studies, Peking University
Beijing 100871 (P. R. China)
E-mail: zhiqi7@pku.edu.cn

Z. Song, Dr. S. Zhong, Prof. L.-J. Qu
State Key Laboratory for Protein and Plant Gene Research
Peking-Tsinghua Center for Life Sciences
College of Life Sciences, Peking University
Beijing 100871 (P. R. China)
E-mail: qulj@pku.edu.cn

Prof. L.-J. Qu
National Plant Gene Research Center
Beijing 100101 (P. R. China)

Supporting information and the ORCID identification number(s) for the author(s) of this article can be found under: https://doi.org/10.1002/anie.201810373.

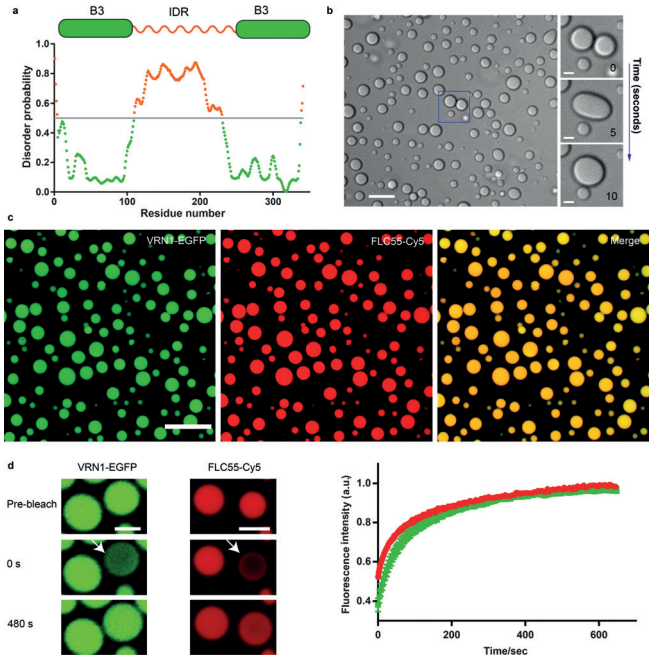

Figure 1. Phase separation of VRN1 with DNA in vitro. a) Residue-specific disorder probability of VRN1 as predicted by PrDOS.[23] b) Left: Purified VRN1 forms spherical droplets with dsDNA FLC55; scale bar: 10 μm. Right: VRN1 droplets undergo fusion; scale bars: 2 μm. c) Phase separation of VRN1–EGFP (20 μM) and FLC55–Cy5 DNA (2 μM); scale bar: 10 μm (left: VRN1–EGFP, middle: FLC55–Cy5, right: merged images). d) Left: Fluorescence intensity recovery of VRN1 droplets after photobleaching; white arrows show bleached droplets; scale bar: 2 μm. Right: Quantification of the fluorescence recovery of VRN1 droplets after bleaching ($N = 3$).

calized in the droplets with a Pearson correlation coefficient of 0.98 (Figure 1c). The results of fluorescence recovery after bleaching (FRAP) showed that both VRN1 and FLC55 fluorescence recovered rapidly with similar speeds after photobleaching (Figure 1d). Bleaching of a section of the droplet gave similar results (see Figure S4). This result indicates the rapid exchange of VRN1 and FLC55 DNA molecules inside and outside the droplets, and shows that the droplets have liquidlike properties.

Protein–DNA interactions are primarily mediated by electrostatic interactions. Therefore, we tested the effect of ionic conditions on the phase separation. As expected, increasing ionic strength reduced the observed phase separation (see Figure S5a). We also tested the effect of 1,6-hexanediol, which is commonly used to detect hydrophobicity-mediated phase separation,[6,22] on the phase separation, but did not detect any changes (see Figure S5b). These results confirmed that electrostatic interactions were the major driving force for the VRN1/DNA phase separation.

Multivalent interactions are considered as the driving force for phase separation. We hypothesized that the two B3 DNA-binding domains in VRN1 were important in protein–DNA multivalent interactions and droplet formation. Therefore, we constructed VRN1 deletion mutants to test the role of these domains in phase separation. We found that the single B3 domain (residues 221–341) could not undergo phase separation with DNA, whereas B3IDR (the B3 domain plus the IDR) weakly demixed with DNA (Figure 2b).

We then studied the concentrations that permitted droplet formation and generated phase diagrams (Figure 2c,d). B3IDR only demixed with DNA at much higher concentrations than VRN1, thus suggesting that multivalent interactions were crucial for complex growth and droplet forma-

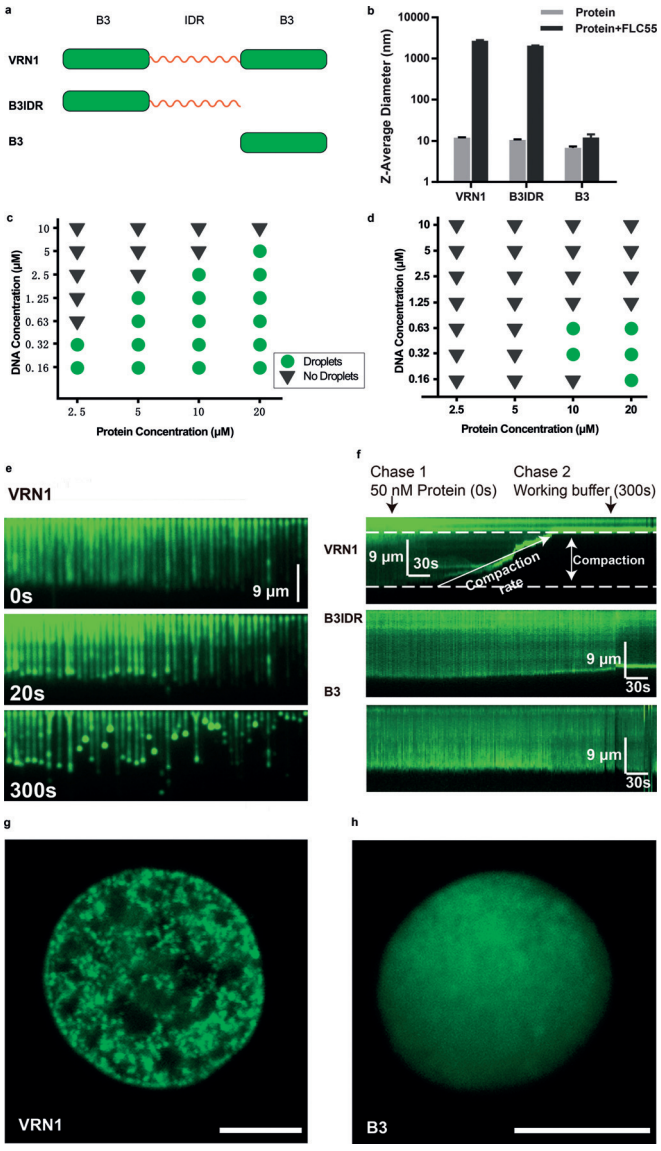

Figure 2. Multivalent interactions drive VRN1 phase separation. a) VRN1 truncations used in this study. b) Dynamic light scattering analysis of particle sizes of the B3 domain, B3IDR, and VRN1 ($N = 3$). c,d) Phase diagrams of FLC55 DNA with VRN1 (c) and B3IDR (d). e) Wide-field total internal reflection fluorescence microscopy (TIRFM) images showing how VRN1 interacted with DNA at the indicated time points. f) Kymographs (400 s) showing how VRN1 (top), BD3 (middle), and BD3IDR (bottom) interacted with DNA in real time. The protein samples reached the flow cell at 0 s (Chase 1, first arrow pointing downward), and the working buffer was exchanged into the flow cell at 300 s (Chase 2, second arrow pointing downward). g) Specklelike puncta formed by VRN1–EGFP in the nucleus of *N. benthamiana* leaf cells; scale bar: 5 μm. h) Even distribution of B3–EGFP inside the nucleus of *N. benthamiana* leaves; scale bar: 5 μm.

tion. We tested whether the DNA valence (proportional to DNA length as VRN1 binds DNA nonspecifically) affected VRN1 phase separation (see Figure S6). The solution turbidity increased with increasing DNA valence at the same protein concentration (see Figure S6). These results suggested that both protein and DNA valency contributed to the multivalent interactions and phase separation.

We further monitored VRN1 phase separation using DNA curtains,[24–26] which is a high-throughput single-molecule technique for direct monitoring of protein–DNA interactions by fluorescence imaging. We established DNA curtains in a flow cell using Lambda DNA (N3011, New England Biolabs). When VRN1 (50 nM) was injected (Figure 2e), the DNA molecules started to shrink, and bright fluorescent puncta were formed at the end of DNA (Figure 2e,f). This shrinking behavior was also observed in a previous study,[5] in which human heterochromatin protein 1α (HP1α) shrank DNA molecules rapidly in DNA curtains and formed LLPS with DNA. In the kymograph in Figure 2f, we define "compaction" as the shrink length of DNA molecules, and "compaction rate" as how fast DNA shrinks. Under treatment with wild-type VRN1, the DNA compaction was (6.1 ± 3.4) μm and the compaction rate was $(63 \pm 35)\ \mathrm{nm\,s^{-1}}$ (see Figure S7c). The VRN1 mutant B3 (Figure 2a) had no observable effect on the length of the DNA molecules (see Figure S7a,c,e). The VRN1 mutant B3IDR (Figure 2a) only shrank DNA slightly with a compaction of (1.3 ± 0.8) μm (see Figure S7b,c, $N = 43$), which is much shorter than that of wild-type VRN1. These results are consistent with the droplet experiments, which indicated that multivalent interactions of VRN1 with DNA are required for phase separation.

VRN1 has a central role in silencing the flowering repressor gene *FLC*. Therefore, phase separation of VRN1 with DNA could be a key process in gene silencing. We transiently expressed the VRN1–EGFP fusion protein in *Nicotiana benthamiana* leaves to test whether the phase separation of VRN1 with DNA occurs in plant cells. The results showed that VRN1–EGFP formed dispersed puncta inside the nucleus (Figure 2g; see also Figure S8a). The puncta fused over time, and the fluorescence intensity was recovered after bleaching (see Figures S9 and S10), thus indicating the liquidlike property of the puncta. As compared to the wild-type VRN1, the single B3 domain of VRN1, which failed to demix with DNA in vitro, did not form puncta in the nucleus (Figure 2h; see also Figure S8b). These results indicated that the multivalent DNA-binding of VRN1 facilitated puncta formation in plant cells, which may affect VRN1-mediated gene repression. How this kind of phase separation is related to the physiological functions of VRN1 needs to be explored in the future.

In addition to the two basic B3 domains, the flexible linker in between also contains several patches of positive or negative charges. We studied the effect of the flexible linker sequence on phase separation. The flexible linker contains several proline–serine/threonine (P-S/T) repeats, and oppositely charged residue patches are segregated. We hypothesized that the basic and acidic patches may be important in determining the protein conformation and its interaction with DNA. Acidic patches may cause DNA repulsion and restrict protein conformation, whereas basic patches may repel the two B3 domains, force a more extended protein conformation, and attract DNA. We extracted these patterns and designed four mutants with altered IDR sequences (Figure 3a). The proline–serine (PS)-neutral mutant (PSN) contains two B3 domains tethered by simple PS repeats, whereas the PS-acidic (PSA) and PS-basic (PSB) mutants contain an acidic or basic patch, respectively. The PS-acidic–basic (PSAB) mutant encompasses both acidic and basic sequence patches in the IDR. We tested whether these four mutants could undergo phase separation with DNA. PSAB formed liquidlike droplets with DNA, similar to the wild-type VRN1 (Figure 3b,c). PSN contained a neutral linker and generated

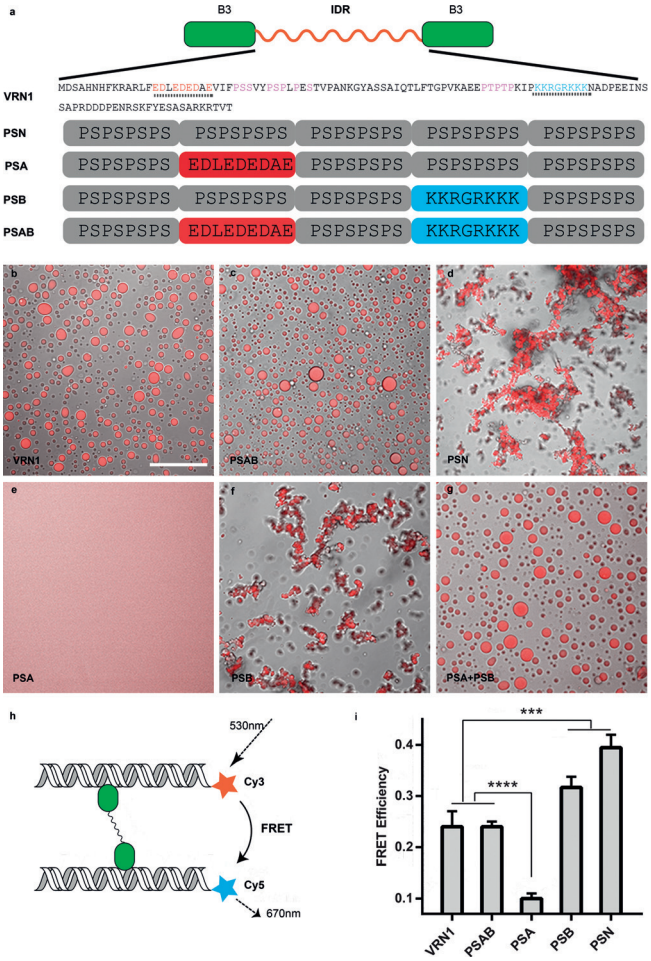

Figure 3. The VRN1 IDR electrostatic pattern significantly contributes to phase separation. a) VRN1 IDR sequence and the four engineered sequences PSN, PSA, PSB, and PSAB. b) VRN1 and DNA form liquidlike droplets; scale bar: 50 μm. c) PSAB and DNA also form liquidlike droplets. d) Charge-deficient PSN forms precipitates with DNA. e) PSA with abundant negative charge does not undergo phase separation with DNA. f) PSB with abundant positive charge forms precipitates with DNA. g) A mixture of PSA and PSB forms liquid droplets with DNA. h) FRET method employed in this study. i) FRET efficiency of Cy3–Cy5 pairs after incubation with each indicated protein. Error bars represent standard deviation ($N = 3$). Distributions were statistically compared using a two-tailed t test; ***$p < 0.001$, ****$p < 0.0001$.

precipitates with DNA (Figure 3d). In contrast, PSA did not demix with DNA, and PSB formed precipitates with DNA similar to PSN (Figure 3e,f). Mixing of equal molar amounts of PSA and PSB generated liquidlike droplets with DNA (Figure 3g), thus suggesting that both the acidic and basic patches in the IDR are important for complex formation and relaxation. We further designed a new sequence by dispersing the positive and negative charges uniformly in the IDR (PSCS). PSCS underwent gel-like aggregation with DNA (see Figure S11), which is similar to the behavior observed for PSN. This result confirmed that both the acidic and the basic residue patches are important for maintaining the right structure of VRN1 for LLPS formation.

To further test how the electrostatic pattern affects the protein–DNA interaction, we performed fluorescence resonance energy transfer (FRET) analysis of phase separation with protein constructs and Cy3 (donor)- and Cy5 (acceptor)-labeled FLC55 (Figure 3h). Equal amounts of labeled DNA were mixed before the addition of each protein construct. The emission intensities of the donor and acceptor were recorded after excitation. The addition of PSA resulted in a low FRET signal, as it did not generate droplets or precipitates with DNA (Figure 3i). VRN1 and PSAB generated medium FRET signals by forming liquidlike droplets with DNA (Figure 3i). In contrast, PSB and PSN generated strong FRET signals by forming condensed precipitates with DNA (Figure 3i). These results indicate that phase separation reduced the intermolecular distance, and precipitates were more compact than liquidlike droplets. We also quantified the fluorescence intensity inside the condensed phase. Except for PSA, which does not condensate with DNA, VRN1 and the other mutants enriched DNA in the condensed phase (see Figure S12). Precipitate-like PSB/DNA and PSN/DNA had higher fluorescence intensity than liquidlike VRN1/DNA and PSAB/DNA. This result is consistent with our FRET data (Figure 3i), which indicated that precipitates were more compact than liquid droplets.

Salts can modulate polyelectrolyte condensation and determine the precipitate–coacervate continuum.[27–29] We further studied the mechanism of PSN- and PSB-mediated precipitate formation. PSN and PSB formed fiberlike precipitates with DNA in the presence of 50 mM KCl (Figure 4a,d), close to the salt concentration in commonly used plant-tissue culture media. The matter state of the separated phase can be tuned by environmental triggers, from spherical liquidlike droplets to amorphous gel-like sticky matter and irregular large precipitates. Increasing the salt concentration to 100 mM generally reduced the size of the precipitates and induced the formation of gel-like material (Figure 4b,e). A further increase of the salt concentration converted the gel-like precipitates to liquidlike droplets (Figure 4c,f). These results indicated that the strength of electrostatic interactions played an important role in regulating the condensation process. Strong electrostatic interactions promoted the formation of solidlike precipitates, and weak electrostatic interactions induced liquid-droplet formation.

In summary, we have shown that the *Arabidopsis* transcriptional regulator VRN1 formed liquidlike spherical droplets with DNA. Both the two B3 DNA binding domains and the disordered linker are essential for phase separation. The IDR tunes the interaction strength between VRN1 and DNA. Increasing the interaction strength, as in the cases of PSN and PSB, induced the formation of solid precipitates, which could be reverted to liquidlike droplets by weakening the interaction strength with a higher salt concentration. We also demonstrated that VRN1 formed liquidlike puncta in plant cell nuclei. Future studies will be necessary to elucidate how VRN1 regulates gene expression and vernalization in *Arabidopsis* through phase separation.

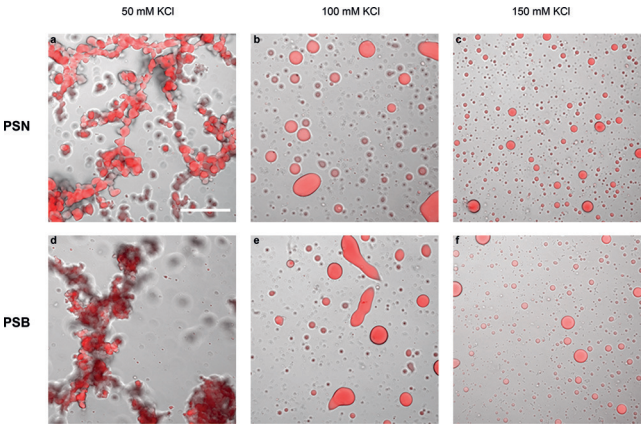

Figure 4. Phase separation of the VRN1 mutants PSN and PSB with increasing salt concentration. a–c) Phase separation of PSN with DNA at the indicated salt concentrations. d–f) Transformation of PSB/DNA precipitates into liquid droplets at the given salt concentrations. Scale bar: 50 μm.

Acknowledgements

This research was supported in part by the Ministry of Science and Technology of China (2015CB910300, 2016YFA0502303) and the National Natural Science Foundation of China (21633001, 31830004, 31621001, and 31670762). We thank Hao Ruan for stimulating discussions and Yan Guan for training and technical assistance with confocal image acquisition.

Conflict of interest

The authors declare no conflict of interest.

Keywords: DNA · intrinsically disordered proteins · multivalent interactions · phase separation · vernalization

How to cite: *Angew. Chem. Int. Ed.* **2019**, *58*, 4858–4862
Angew. Chem. **2019**, *131*, 4912–4916

[1] J. E. Phillips-Cremins et al., *Cell* **2013**, *153*, 1281–1295.
[2] Y. Li, M. Hu, Y. Shen, *Hum. Mol. Genet.* **2018**, https://doi.org/10.1093/hmg/ddy164.
[3] D. Hnisz, K. Shrinivas, R. A. Young, A. K. Chakraborty, P. A. Sharp, *Cell* **2017**, *169*, 13–23.
[4] B. R. Sabari et al., *Science* **2018**, *361*, eaar3958.

[5] A. G. Larson, D. Elnatan, M. M. Keenen, M. J. Trnka, J. B. Johnston, A. L. Burlingame, D. A. Agard, S. Redding, G. J. Narlikar, *Nature* **2017**, *547*, 236 – 240.
[6] A. R. Strom, A. V. Emelyanov, M. Mir, D. V. Fyodorov, X. Darzacq, G. H. Karpen, *Nature* **2017**, *547*, 241 – 245.
[7] A. L. Turner, M. Watson, O. G. Wilkins, L. Cato, A. Travers, J. O. Thomas, K. Stott, *Proc. Natl. Acad. Sci. USA* **2018**, *115*, 11964 – 11969.
[8] X. Su, J. A. Ditlev, E. Hui, W. Xing, S. Banjade, J. Okrut, D. S. King, J. Taunton, M. K. Rosen, R. D. Vale, *Science* **2016**, *352*, 595 – 599.
[9] J. A. Riback, C. D. Katanski, J. L. Kear-Scott, E. V. Pilipenko, A. E. Rojek, T. R. Sosnick, D. A. Drummond, *Cell* **2017**, *168*, 1028 – 1040.e19.
[10] P. Li, *Nature* **2012**, *483*, 336 – 340.
[11] D. M. Mitrea, J. A. Cika, C. B. Stanley, A. Nourse, P. L. Onuchic, P. R. Banerjee, A. H. Phillips, C.-G. Park, A. A. Deniz, R. W. Kriwacki, *Nat. Commun.* **2018**, *9*, https://doi.org/10.1038/s41467-018-03255-3.
[12] M. Zeng, Y. Shang, Y. Araki, T. Guo, R. L. Huganir, M. Zhang, *Cell* **2016**, *166*, 1163 – 1175.e12.
[13] R. J. Cohen, G. B. Benedek, *J. Phys. Chem.* **1982**, *86*, 3696 – 3714.
[14] S. F. Banani, A. M. Rice, W. B. Peeples, Y. Lin, S. Jain, R. Parker, M. K. Rosen, *Cell* **2016**, *166*, 651 – 663.
[15] S. F. Banani, H. O. Lee, A. A. Hyman, M. K. Rosen, *Nat. Rev. Mol. Cell Biol.* **2017**, *18*, 285 – 298.
[16] Y. Lin, D. S. W. Protter, M. K. Rosen, R. Parker, *Mol. Cell* **2015**, *60*, 208 – 219.
[17] Y. Shin, C. P. Brangwynne, *Science* **2017**, *357*, eaaf4382.
[18] Y. Y. Levy, *Science* **2002**, *297*, 243 – 246.
[19] R. Bastow, J. S. Mylne, C. Lister, Z. Lippman, R. A. Martienssen, C. Dean, *Nature* **2004**, *427*, 164 – 167.
[20] J. S. Mylne, L. Barrett, F. Tessadori, S. Mesnage, L. Johnson, Y. V. Bernatavichute, S. E. Jacobsen, P. Fransz, C. Dean, *Proc. Natl. Acad. Sci. USA* **2006**, *103*, 5012 – 5017.
[21] G. J. King, A. H. Chanson, E. J. McCallum, M. Ohme-Takagi, K. Byriel, J. M. Hill, J. L. Martin, J. S. Mylne, *J. Biol. Chem.* **2013**, *288*, 3198 – 3207.
[22] S. Kroschwald, S. Maharana, A. Simon, *Matters* **2017**, https://doi.org/10.19185/matters.201702000010.
[23] T. Ishida, K. Kinoshita, *Nucleic Acids Res.* **2007**, *35*, W460 – W464.
[24] E. C. Greene, S. Wind, T. Fazio, J. Gorman, M.-L. Visnapuu in *Methods in Enzymology*, Elsevier, Amsterdam, **2010**, pp. 293 – 315.
[25] Z. Qi, E. C. Greene, *Methods* **2016**, *105*, 62 – 74.
[26] Y. Zhao, Y. Jiang, Z. Qi, *J. Phys. D* **2017**, *50*, 153001.
[27] R. Chollakup, J. B. Beck, K. Dirnberger, M. Tirrell, C. D. Eisenbach, *Macromolecules* **2013**, *46*, 2376 – 2390.
[28] Q. Wang, J. B. Schlenoff, *Macromolecules* **2014**, *47*, 3108 – 3116.
[29] S. Ali, V. Prabhu, *Gels* **2018**, *4*, 11.

Manuscript received: September 9, 2018
Accepted manuscript online: February 14, 2019
Version of record online: March 12, 2019

